NEOPLASIA
www.neoplasia.com
Volume 15 Number 10 October 2013 pp. 1161–1171 1161

Allosteric MEK1/2 Inhibitor Refametinib (BAY 86-9766) in Combination with Sorafenib Exhibits Antitumor Activity in Preclinical Murine and Rat Models of Hepatocellular Carcinoma[1,2]

Roberta Schmieder[*,3], Florian Puehler[*,3], Roland Neuhaus[*], Maria Kissel[*], Alex A. Adjei[†], Jeffrey N. Miner[‡], Dominik Mumberg[*], Karl Ziegelbauer[*] and Arne Scholz[*]

[*]Global Drug Discovery, Bayer HealthCare, Berlin, Germany;
[†]Roswell Park Cancer Institute, Buffalo, NY;
[‡]Ardea Biosciences, Inc, San Diego, CA

Abstract

OBJECTIVE: The objectives of the study were to evaluate the allosteric mitogen-activated protein kinase kinase (MEK) inhibitor BAY 86-9766 in monotherapy and in combination with sorafenib in orthotopic and subcutaneous hepatocellular carcinoma (HCC) models with different underlying etiologies in two species. *DESIGN:* Antiproliferative potential of BAY 86-9766 and synergistic effects with sorafenib were studied in several HCC cell lines. Relevant pathway signaling was studied in MH3924a cells. For *in vivo* testing, the HCC cells were implanted subcutaneously or orthotopically. Survival and mode of action (MoA) were analyzed. *RESULTS:* BAY 86-9766 exhibited potent antiproliferative activity in HCC cell lines with half-maximal inhibitory concentration values ranging from 33 to 762 nM. BAY 86-9766 was strongly synergistic with sorafenib in suppressing tumor cell proliferation and inhibiting phosphorylation of the extracellular signal–regulated kinase (ERK). BAY 86-9766 prolonged survival in Hep3B xenografts, murine Hepa129 allografts, and MH3924A rat allografts. Additionally, tumor growth, ascites formation, and serum alpha-fetoprotein levels were reduced. Synergistic effects in combination with sorafenib were shown in Huh-7, Hep3B xenografts, and MH3924A allografts. On the signaling pathway level, the combination of BAY 86-9766 and sorafenib led to inhibition of the upregulatory feedback loop toward MEK phosphorylation observed after BAY 86-9766 monotreatment. With regard to the underlying MoA, inhibition of ERK phosphorylation, tumor cell proliferation, and microvessel density was observed *in vivo*. *CONCLUSION:* BAY 86-9766 shows potent single-agent antitumor activity and acts synergistically in combination with sorafenib in preclinical HCC models. These results support the ongoing clinical development of BAY 86-9766 and sorafenib in advanced HCC.

Neoplasia (2013) 15, 1161–1171

Abbreviations: HCC, hepatocellular carcinoma; HBV, hepatitis B virus; HCV, hepatitis C virus; VEGFRs, vascular endothelial growth factor receptors; OS, overall survival; AFP, alpha-fetoprotein

Address all correspondence to: Florian Puehler, PhD, Bayer Pharma AG, Muellerstr. 178, 13353 Berlin, Germany. E-mail: florian.puehler@bayer.com

[1]This work was supported by Bayer HealthCare (Berlin, Germany) and Ardea Biosciences (San Diego, CA). Writing assistance was provided by Synapse Medical Communications (New York, NY). R.S., F.P., R.N., M.K., D.M., K.Z., and A.S. are stockholders and/or employees of Bayer Pharma AG. Prior presentations: Part of this work was presented at the American Association for Cancer Research–National Cancer Institute–European Organisation for Research and Treatment of Cancer meeting in San Francisco on November 12 to 16, 2011.
[2]This article refers to supplementary materials, which are designated by Figures W1 to W3 and are available online at www.neoplasia.com.
[3]These authors contributed equally to this work.
Received 22 April 2013; Revised 9 September 2013; Accepted 9 September 2013

DOI 10.1593/neo.13812

Introduction

Hepatocellular carcinoma (HCC) is the major histologic subtype of primary liver cancer, accounting for 70% to 85% of cases in most countries [1]. In 2008, liver cancer was diagnosed in an estimated 748,300 people and was responsible for an estimated 695,900 deaths, with the highest rates found in eastern and southeastern Asia and in central and western Africa [2]. Although liver cancer is less common in Europe than in parts of Asia and Africa, the incidence in the West is increasing [2,3].

High 5-year survival rates can be achieved in selected patients with preserved liver function by using partial hepatectomy in early-stage HCC, ablative therapy in locoregional disease, and liver transplantation in unresectable disease [4]. However, HCC constitutes a significant unmet medical need because of the high proportion of patients diagnosed with advanced cancer, as well as the high rates of disease progression following locoregional therapy. Adding to the complexity, HCC typically occurs in patients having one of several underlying liver diseases, most commonly chronic infection with hepatitis B virus (HBV) or hepatitis C virus (HCV).

The mitogen-activated protein kinase pathway—also known as the RAS/RAF/MEK/extracellular signal-regulated kinase (ERK) pathway [MAP kinase (MAPK) pathway]—is a ubiquitous intracellular cascade that transduces signals from cell surface receptors to regulate numerous cytoplasmic and nuclear proteins involved in cellular proliferation, survival, differentiation, migration, and angiogenesis [5–7]. Unlike other solid tumors, mutations in the *RAS* and *RAF* genes are rarely found in HCC [8,9]. Instead, overexpression of RAS, down-regulation of the natural inhibitors of the MAPK pathway, and overexpression of MEK and ERK are the mechanisms of MAPK pathway activation in HCC [10–14]. Moreover, ERK overexpression has been correlated with disease progression in HCC [15].

HBV and HCV may increase risk of HCC through activation of the MAPK pathway. After integration of HBV DNA into the human genome, two viral transcription factors (HBx and PreS2 activator) are expressed, which stimulate MAPK pathway signaling, leading to cellular proliferation and transformation [16].

Early aspects of alcohol-induced liver damage appear associated with activation of key signaling pathways, including ERK1/2, which in turn drives increased expression of various transduction factors, such as sterol regulatory element binding proteins and early growth factor response 1 [17]. Physiologically relevant concentrations of ethanol, corresponding to blood alcohol levels of 0.05 to 0.18 mg/dl, increase transforming growth factor α levels, leading to activation of MEK and ERK signaling, cell cycle progression, and cell proliferation in human HCC cell lines but not in normal human hepatocytes [18].

A recent study has analyzed the phospho-ERK1/2 (pERK1/2) levels in tumor tissue from patients with HCC related to HBV, HCV, and chronic alcohol abuse. In patients with HCV infection, 51.9% (27 of 52) showed high pERK levels, 20% (8 of 40) of patients with HBV had elevated pERK expression levels, and 37.9% (11 of 29) of patients with ethanol abuse exhibited increased pERK1/2 staining [19].

Sorafenib is a multikinase inhibitor that targets receptor tyrosine kinases; vascular endothelial growth factor receptors (VEGFRs) 1, 2, and 3; platelet-derived growth factor β; Fms-related tyrosine kinase 3 (FLT-3); Ret; c-Kit; and serine/threonine kinases RAF-1 and B-RAF [20,21]. Due to its antiproliferative, antiangiogenic, and proapoptotic effects, sorafenib is a compound with a potent antitumoral efficacy.

In the phase III Sorafenib Hepatocellular Carcinoma Assessment Randomized Protocol trial, sorafenib significantly improved overall survival (OS) and time to progression compared with placebo in patients with advanced HCC [22]. Sorafenib also improved OS and time to progression in another phase III trial that enrolled only Asian patients with advanced HCC [23]. On the basis of these trials, sorafenib is currently the standard of care for HCC patients with Child-Pugh class A liver function who have metastatic disease or unresectable disease not amenable to liver transplantation [24].

BAY 86-9766 (Refametinib; previously RDEA119) is a highly selective and potent orally available inhibitor of MEK 1 and MEK 2. The structural, pharmacologic, and pharmacokinetic properties of BAY 869766 are described in detail in the paper by Iverson et al. [25]. In a panel of more than 200 tested kinases, only the enzymes MEK1/2 were inhibited significantly, through the allosteric binding of BAY 86-9766. The MEK inhibitor BAY 86-9766 displays potent *in vitro* and *in vivo* antitumor activity in multiple preclinical cancer models, including melanoma, colorectal cancer, non–small cell lung cancer, epidermal carcinoma, and HCC [21,25], and is currently in phase I and II clinical trials for various solid tumors.

In the present report, BAY 86-9766 was evaluated as monotherapy and in combination with sorafenib in four different HCC models. To reproduce the biology of human cancer as closely as possible, we chose three orthotopic models. In contrast to commonly used subcutaneous xenografts, orthotopic models reflect the importance of the tumor microenvironment. They allow the interaction of organ-specific factors (for example, fibroblasts, endothelial cells, and inflammatory cells) with tumor cells [26,27]. These models show metastatic spread and a higher degree of vascularity compared with ectopic tumors. All of these mechanisms, which are also important in human HCC development, can be tested only in orthotopic models. In addition, the immune system might also play a role in response to HCC therapy. To evaluate possible immunologic effects, two of the four models are syngeneic: the murine Hepa129 model and the MH3924A rat model.

The human Hep3B model, which is HBV driven, was chosen in recognition of the fact that three fourths of all liver cancer deaths are attributed to hepatitis B infection worldwide [28].

Furthermore, we have characterized on the molecular level differences in the MAPK pathway inhibition profile for sorafenib and BAY 86-9766 in monotreatment and combination treatment.

Materials and Methods

Cell Proliferation Assays

All cell lines were plated in 96-well plates and incubated overnight at 37°C. For the time zero determination, CellTiter-Glo reagent (Promega Corporation, Madison, WI) was added to the wells on a sister plate. The plates were analyzed on a VICTOR^3 plate reader (PerkinElmer Inc, Waltham, MA). Twenty-four hours after cell seeding, test compounds, which were evaluated in serial dilutions at concentrations ranging from 300 pM to 10 μM, were added to the wells. Cells were incubated for 72 hours at 37°C before the CellTiter-Glo luminescence signal was determined on a VICTOR X3 plate reader. The percentage change in cell growth was calculated by normalizing the measurements to the extinctions of the time zero point plate (=0%) and the untreated (0 μM) cells (=100%). The half-maximal inhibitory concentrations (IC_{50}) were determined by means of a four-parameter fit using MTS Software (Bayer Software, Berlin, Germany).

Analysis of Combination Effects

The combination effects of BAY 86-9766 and sorafenib in the 72-hour cell proliferation assay were evaluated using combination

index isobologram analysis. Briefly, cells were plated onto a 384-well plate with 25 µl of medium. After a 24-hour incubation at 37°C, 5 µl of medium containing BAY 86-9766 (D1), sorafenib (D2), or the combination of both compounds at different ratios (0.9 × D1 + 0.1 × D2, 0.7 × D1 + 0.3 × D2, 0.5 × D1 + 0.5 × D2, 0.3 × D1 + 0.7 × D2, and 0.1 × D1 + 0.9 × D2) was used to make serial threefold dilutions to generate seven concentration-response curves. Each experiment was conducted in triplicate.

The mapping of the ratio of half-maximal effective concentration to half-maximal inhibitory concentration (EC_{50}/IC_{50}) was determined by means of a four-parameter fit using MTS Software (Bayer Software). The corresponding component doses of BAY 86-9766 and sorafenib at the EC_{50}/IC_{50} were calculated and used for plotting isobolograms. Multiple-drug effect was analyzed as described by Chou [29], and the combination index was calculated using the following formula: Combination index = [D1x]/D1′ + [D2x]/D2′, where D1x and D2x refer to the drug 1 and drug 2 concentration at the EC_{50}/IC_{50} in combination, and D1′ and D2′ refer to the EC_{50}/IC_{50} values of D1 and D2, respectively, as a single agent. In this analysis, combination indexes of 0 to 0.3, 0.3 to 0.6, and 0.6 to 0.9 were defined as very strong synergy, strong synergy, and synergy, respectively.

Orthotopic Hep3B HCC Xenograft

Human HBV-driven Hep3B HCC cells were implanted orthotopically onto female Naval Medical Research Institute (NMRI) nude mice. Treatment was started on day 8 following implantation with once daily single-agent BAY 86-9766 (5 or 25 mg/kg), once daily sorafenib (maximum tolerated dose of 30 mg/kg), or combination of BAY 86-9766 and sorafenib at same doses. Each regimen was administered to 12 or 13 mice. A control group received vehicle. Levels of HCC serum marker alpha-fetoprotein (AFP) were determined on days 26 and 42 postimplantation when all animals were still alive. The primary end point in this model was median survival, which was determined by Kaplan-Meier analysis.

Allograft Models

Orthotopic rat MH3924A allografts. Female August Copenhagen Irish (ACI) rats were housed and maintained in accordance with Bayer Institutional Animal Care. For induction of orthotopic HCC tumors, rat MH3924A cells (3×10^6) in 50% BD Matrigel (BD Biosciences, San Diego, CA) were injected into the liver under total body anesthesia. The rats were randomly divided into four treatment groups, each containing 18 animals. Treatment was started 10 days after tumor cell injection, at which time the animals showed distinct tumor growth. BAY 86-9766 (3 mg/kg) and sorafenib (6 mg/kg), or their corresponding vehicles, were administered orally once daily at least 4 hours apart. After the first animal in the vehicle group died, six rats from each group were killed and dissected to evaluate primary tumor weight and metastatic spread and to collect tumor samples for immunohistochemical staining. The remaining 12 rats in each group were followed to determine median survival.

For pharmacokinetic (PK) analysis, sorafenib was administered 5.75 hours after BAY 86-9766, and blood samples for analysis of plasma BAY 86-9766 and sorafenib concentrations were collected before and 0.5, 1, 2, 5, 8, and 24 hours after dosing of BAY 86-9766 on day 14. Samples were collected from a venous catheter into tubes containing lithium heparin and then centrifuged to isolate the plasma, which was stored at −20°C until analysis. Samples were analyzed after precipitation with acetonitrile (1/5, vol/vol) using an Agilent 1200 HPLC with liquid chromatography/mass spectrometry/mass spectrometry (LC/MS/MS) detection. Drug concentrations were quantified by calibration with a standard curve and an internal standard.

Orthotopic Hepa129 HCC allografts. Murine Hepa129 HCC cells (5×10^5) were implanted orthotopically into the liver female C3H/He mice. Treatment with BAY 86-9766 (25 mg/kg, once daily) or vehicle was started 4 days after implantation. Each group contained 10 mice. Starting on day 18, the daily dose of BAY 86-9766 was reduced to 12.5 mg/kg due to slight body weight loss. The mice were followed to determine median survival by Kaplan-Meier analysis.

Statistical Methods

Statistical analyses were performed using GraphPad Prism 5. In the Kaplan-Meier curves, fractional survival (Y) was plotted as a function of time (X) and groups were compared using the log-rank test using a significance level of .05. In case of multiple comparisons, a P level correction was carried out using the Bonferroni method.

For the comparison of immunohistochemistry (IHC) results, tumor and liver weight, Bonforroni multiple comparison test was used, a very conservative but proper method in case of comparing only a few groups.

Western Blot Analysis and Immunohistochemistry from MH3924A Cells and Allograft

See Supplementary Materials and Methods section.

Results

Antiproliferative Activity of BAY 86-9766 as Single Agent

BAY 86-9766 was tested as a single agent in HCC cell lines of different etiologies (Table 1). In each cell line, BAY 86-9766 inhibited cell proliferation *in vitro* in a concentration-dependent manner with greater potency against human HepG2 cells with *NRAS* mutations (IC_{50} = 33 nM) than against human Hep3B and PLC/PRF/5 cells with underlying HBV infection (IC_{50} = 366 and 762 nM, respectively). In comparison, BAY 86-9766 was equipotent with another MEK inhibitor (AZD6244) in the HepG2 cells but three to four times more potent in the other cell lines. Besides the human HCC lines, BAY 86-9766 exhibited a concentration-dependent antiproliferative activity in MH3924A and Hepa129 cells, with IC_{50} values of 540 and 502 nM, respectively.

Strong Synergism between BAY 86-9766 and Sorafenib in Terms of Antiproliferative Effects and Feedback Regulation

As a method of choice to measure *in vitro* synergy, the combination index isobologram analysis has been performed as described in

Table 1. Antiproliferative Activity of the MEK Inhibitors BAY 86-9766 and AZD6244 in HCC Cell Lines.

Cell Line	Species	Etiology/Genetic Mutation	IC_{50} (nM)	
			BAY 86-9766	AZD6244
PLC/PRF/5	Human	HBV infection	762	3060
Hep3B	Human	HBV infection	366	1093
HepG2	Human	*NRAS* mutation	33	32
MH3924A	Rat	Not determined	540	4595
Hepa129	Mouse	Not determined	502	2260

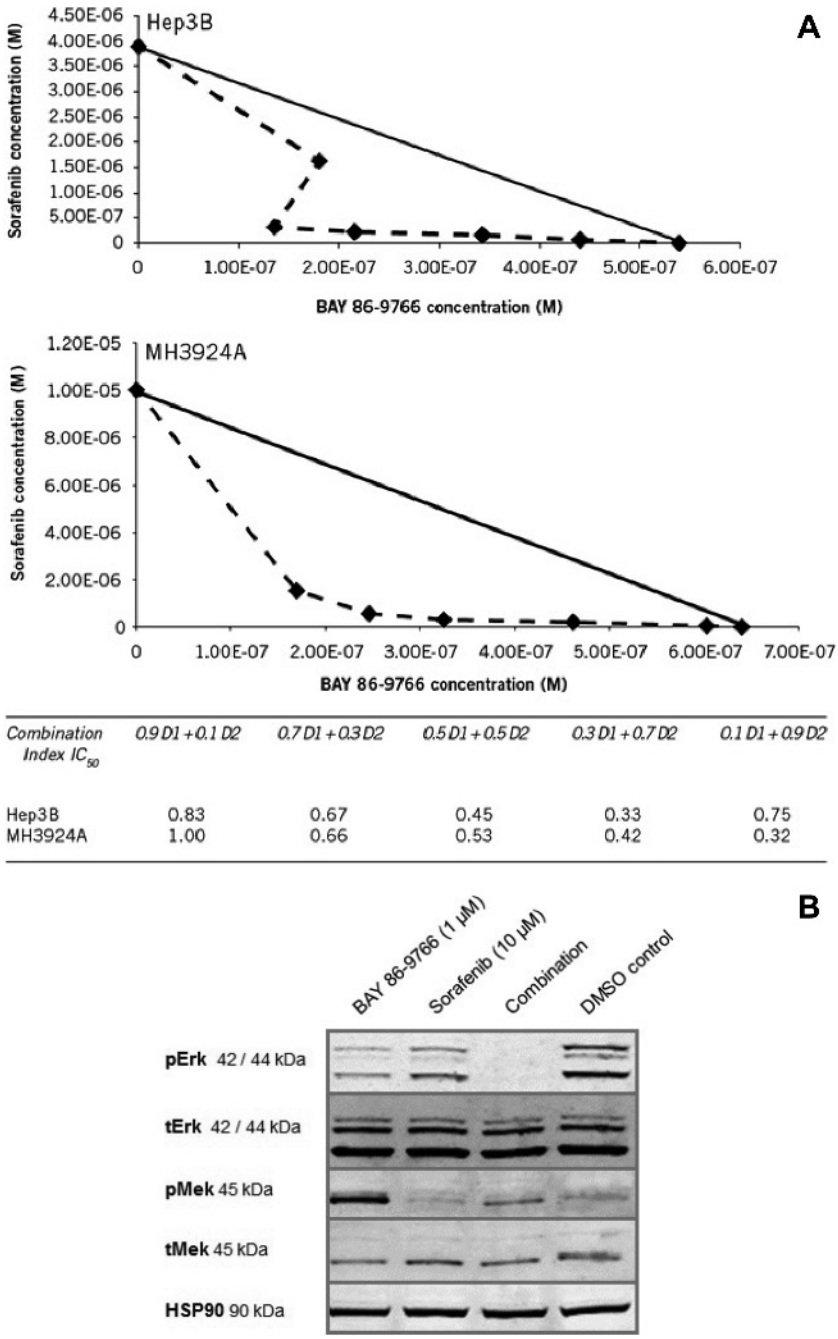

Combination Index IC_{50}	0.9 D1 + 0.1 D2	0.7 D1 + 0.3 D2	0.5 D1 + 0.5 D2	0.3 D1 + 0.7 D2	0.1 D1 + 0.9 D2
Hep3B	0.83	0.67	0.45	0.33	0.75
MH3924A	1.00	0.66	0.53	0.42	0.32

Figure 1. Synergistic antiproliferative activity of BAY 86-9766 and sorafenib in HCC cell lines. Isobologram analysis of the interaction between BAY 86-9766 and sorafenib in human Hep3B cells and rat MH3924A cells is shown in A. Points below the straight diagonal line indicate a synergistic interaction. The combination index analysis for the interaction between the two drugs in these HCC lines is also shown in A (D1, sorafenib; D2, BAY 86-9766). Effects of BAY 86-9766 and sorafenib, as single agents and in combination, in MH3924A cells are shown in B. Phosphorylation of ERK was more potently blocked due to combination treatment in comparison to BAY 86-9766 and sorafenib monotreatment after 12 hours of compound incubation. Additionally, compensatory up-regulation of phosphorylated MEK was diminished in the combination-treated cells.

Materials and Methods section. If the combination data points fall on the hypotenuse, an additive effect is present. If the combination data points fall on the lower left or on the upper right, synergism or antagonism is indicated, respectively. BAY 86-9766 showed synergistic antiproliferative activity when tested in combination with sorafenib in human Hep3B cells (Figure 1*A*). Strong synergism, defined by a combination index of 0.3 to 0.6, was observed for two dose combinations: 0.3 μM BAY 86-9766 + 0.7 μM sorafenib (combination index = 0.33) and 0.5 μM BAY 86-9766 + 0.5 μM sorafenib (combination index = 0.45; Figure 1*A*). The other three dose combinations also exhibited synergy, with the combination index in the range of 0.6 to 0.9. The interaction between BAY 86-9766 and sorafenib was also explored in the rat MH3924A HCC cell line (Figure 1*A*). Strong synergistic antiproliferative activity was evident at four of the five dose combinations, including the two dose combinations with strong synergism in the Hep3B cells.

ERK and MEK phosphorylation was examined in MH3924A cells and visualized by Western blot analysis. Due to combination treatment with BAY 86-9766 and sorafenib, phosphorylation of ERK was completely blocked after 12 hours in comparison to monotherapy. In addition, compensatory up-regulation of phosphorylated MEK signal after BAY 86-9766 monotreatment was diminished in cells treated with combination of both agents (Figure 1*B*).

Efficacy of BAY 86-9766 as Monotherapy and in Combination with Sorafenib in HCC Xenograft Models

Single-agent BAY 86-9766 (20 mg/kg) caused a small inhibition in the growth of subcutaneous human Huh-7 HCC xenografts, which was nearly identical to the growth inhibition observed with sorafenib (50 mg/kg). In contrast, substantial tumor growth inhibition was observed when BAY 86-9766 was administered in combination with sorafenib. At the last assessment, the combination reduced tumor volume by 70% compared with vehicle-treated control animals, whereas the two drugs individually reduced tumor volume by approximately 20%. These results indicate that the combination of BAY 86-9766 and sorafenib produces synergistic tumor growth inhibition in Huh-7 xenografts (data not shown).

In the orthotopic HBV-driven human Hep3B xenograft model, BAY 86-9766 (25 mg/kg) monotherapy was more effective than sorafenib at its maximally tolerated dose (30 mg/kg) in prolonging survival, reducing serum AFP levels and exhibiting strong synergism in improving these end points when combined with sorafenib (Figures 2*A* and W1). Median survival in the group treated with BAY 86-9766 at a daily dose of 25 mg/kg was 60 days, compared with 52 days in the sorafenib group. When BAY 86-9766 (25 mg/kg) and sorafenib were administered in combination, median survival was extended to 80 days—an increase of 70% relative to the vehicle control—which was significantly greater than the median survival in all other groups ($P = .003$, significance level corrected for multiple comparisons using the Bonferroni method; $P = .0008$ by the log-rank

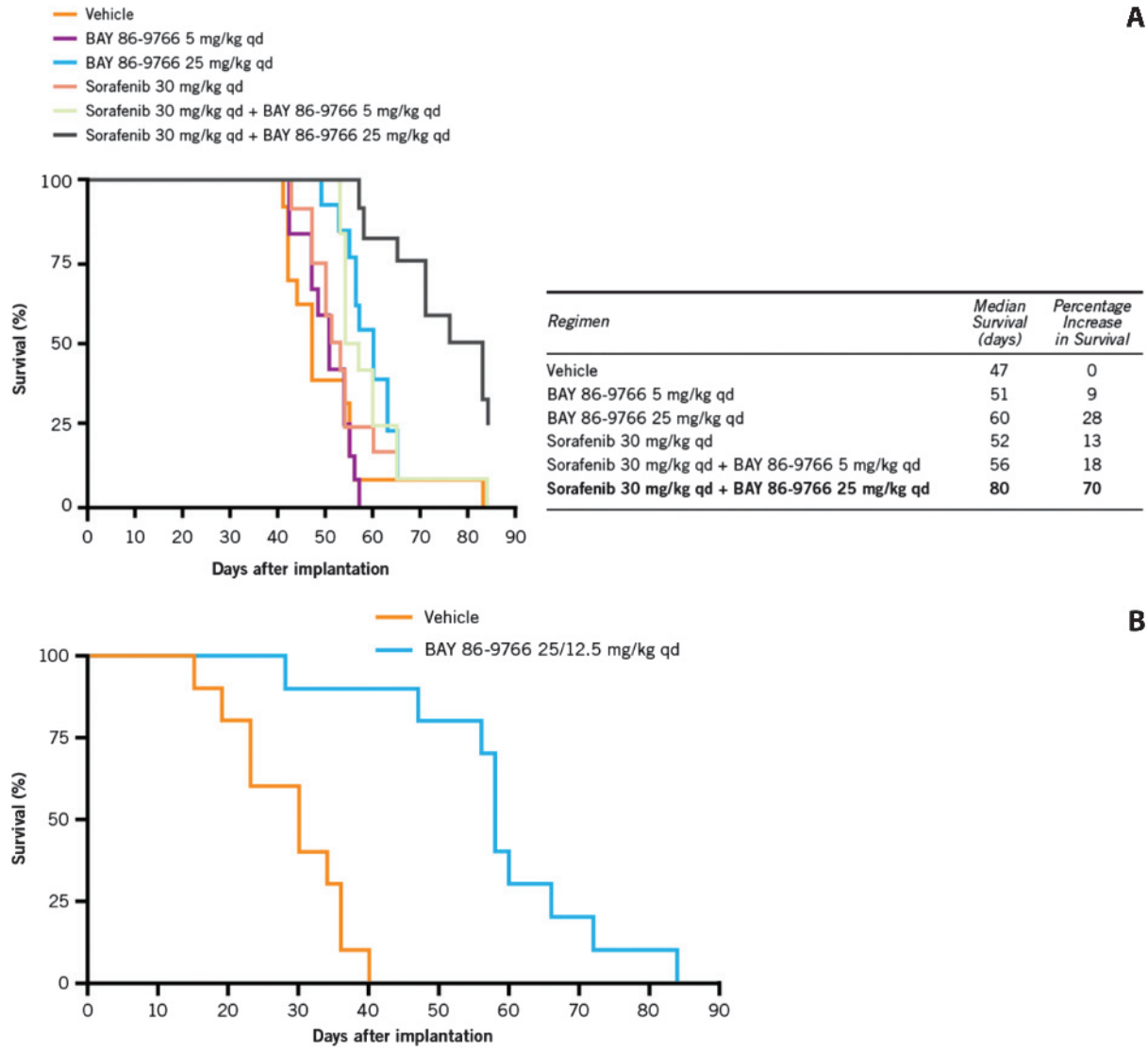

Regimen	*Median Survival (days)*	*Percentage Increase in Survival*
Vehicle	47	0
BAY 86-9766 5 mg/kg qd	51	9
BAY 86-9766 25 mg/kg qd	60	28
Sorafenib 30 mg/kg qd	52	13
Sorafenib 30 mg/kg qd + BAY 86-9766 5 mg/kg qd	56	18
Sorafenib 30 mg/kg qd + BAY 86-9766 25 mg/kg qd	**80**	**70**

Figure 2. Effect of BAY 86-9766 and sorafenib, as single agents and in combination, in the orthotopic HBV-driven human Hep3B xenograft model. Kaplan-Meier survival curves and results are presented in A; comparison of survival with BAY 86-9766 monotherapy *versus* vehicle in the orthotopic murine Hepa129 HCC allograft model is presented in B.

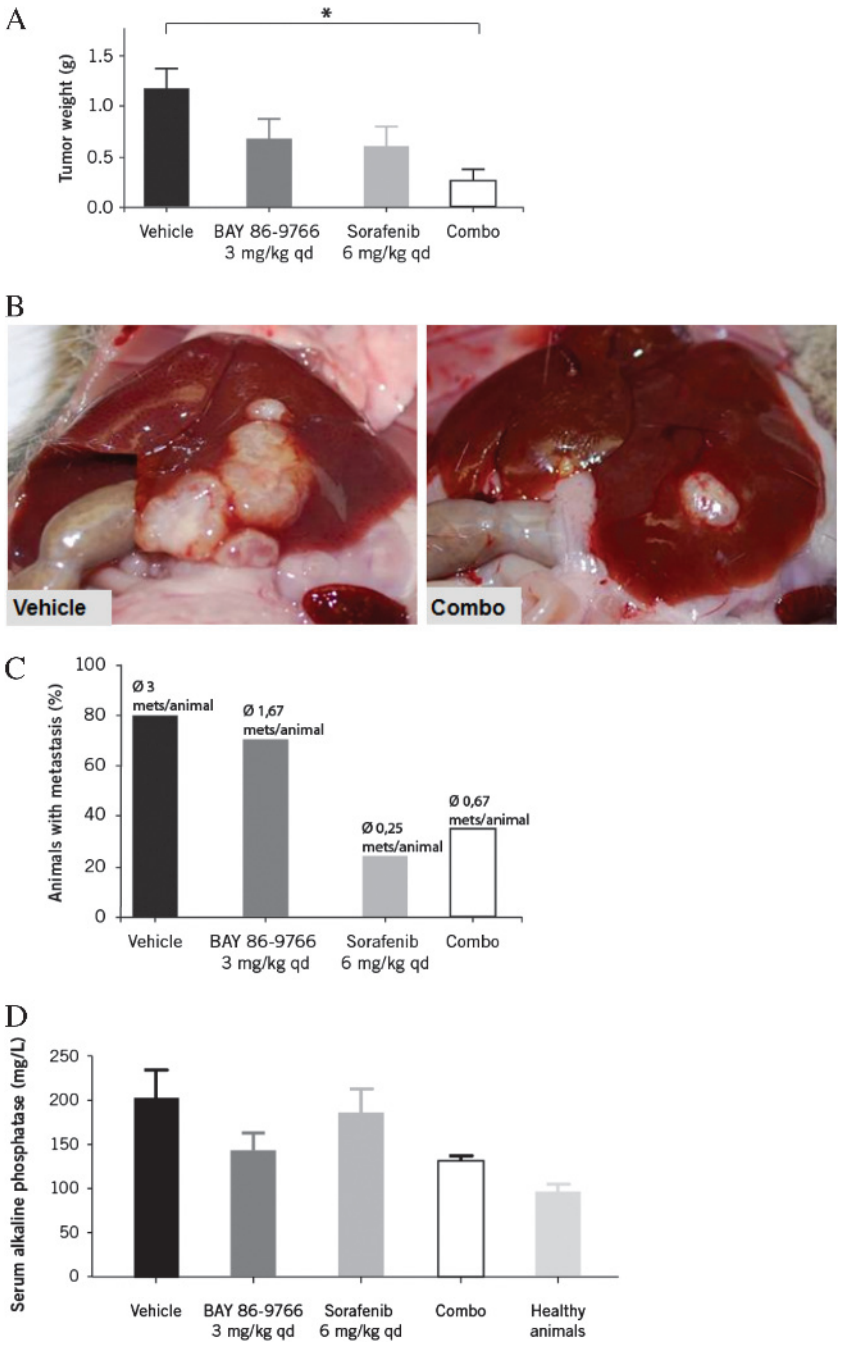

Figure 3. Effect of BAY 86-9766 and sorafenib, as single agents and in combination, on tumor growth, metastatic spread, and alkaline phosphatase levels in the orthotopic rat MH3924A allograft model. The primary tumor, which has been cut out and measured on day 21 following orthotopic implantation, is depicted in A. Significance is indicated by asterisk ($P < .05$). Representative photos of the primary tumor from rats treated with vehicle control or combination therapy are shown in B. The percentage of animals with metastases is presented in C. Mean (+SD) serum alkaline phosphatase levels are shown in D.

test). Of note, long-term treatment (up to 55 days) with the combination was well tolerated. Body weight loss in the group was below 10%, demonstrating long-term tolerability with treatment.

Serum AFP measured on day 26 mirrored the survival results, with the lowest levels seen in the group receiving BAY 86-9766 (25 mg/kg) plus sorafenib followed by the group receiving the same dose of BAY 86-9766 as monotherapy (data not shown). These two groups were also the ones with the lowest serum AFP levels on day 42 (Figure W1). However, significant between-group differences in AFP levels on day 26 or 42 were not seen in multiple comparison statistical tests.

Efficacy of BAY 86-9766 as Monotherapy and in Combination with Sorafenib in HCC Allograft Models

Single-agent BAY 86-9766 significantly prolonged median survival in the orthotopic murine Hepa129 HCC allograft model. Treatment was started on day 4 following implantation at a dose of 25 mg/kg, once daily, but the dose was reduced to 12.5 mg/kg, once daily, starting on day 18 after borderline weight loss was observed. With this regimen, median survival was 58 days in the BAY 86-9766 group compared with 30 days for the vehicle-treated animals ($P < .0001$ by log-rank test; Figure 2*B*).

Single-agent BAY 86-9766 [3 mg/kg; maximal tolerated dose (MTD) determined in the rat model] and single-agent sorafenib (6 mg/kg; MTD determined in the rat model) reduced primary tumor weight compared with vehicle control in the orthotopic rat MH3924A allograft model (not reaching statistical significance; Figure 3*A*). In comparison, combination therapy with BAY 86-9766 and sorafenib produced significant tumor growth inhibition compared with vehicle control (mean primary tumor weight: 0.24 *vs* 1.14 g; $P < .05$ by Bonferroni multiple comparison test). All animals in the control group had tumors ≥0.8 g, whereas 33%, 25%, and 60% of the animals had primary tumors ≤0.2 g in the BAY 86-9766, sorafenib, and combination groups, respectively. The reductions in primary tumor growth were mirrored by significant decreases in liver weight (Figure W2). Median liver weight expressed as a percentage of body weight was 3.2% in the BAY 86-9766 group, 2.8% in the sorafenib group, and 2.5% in the combination group compared with 4.0% in the vehicle control group ($P < .05$ for all comparisons *vs* control by Bonferroni multiple comparison test).

In the MH3924A allograft model, most animals in the control and single-agent BAY 86-9766 groups had evidence of tumor metastases, whereas the lowest rates of metastatic spread were seen in the sorafenib and combination therapy groups (Figure 3*C*). A similar profile was evident when the number of metastases per animal was analyzed: Animals in the control group had a mean of three metastatic sites, whereas a mean of less than one site per animal was found in the sorafenib and combination therapy groups. However, neither the incidence of tumor metastases nor the number of metastases per animal differed significantly across treatment groups. Ascites was detected in 60% of the control animals but in none of the animals in the other

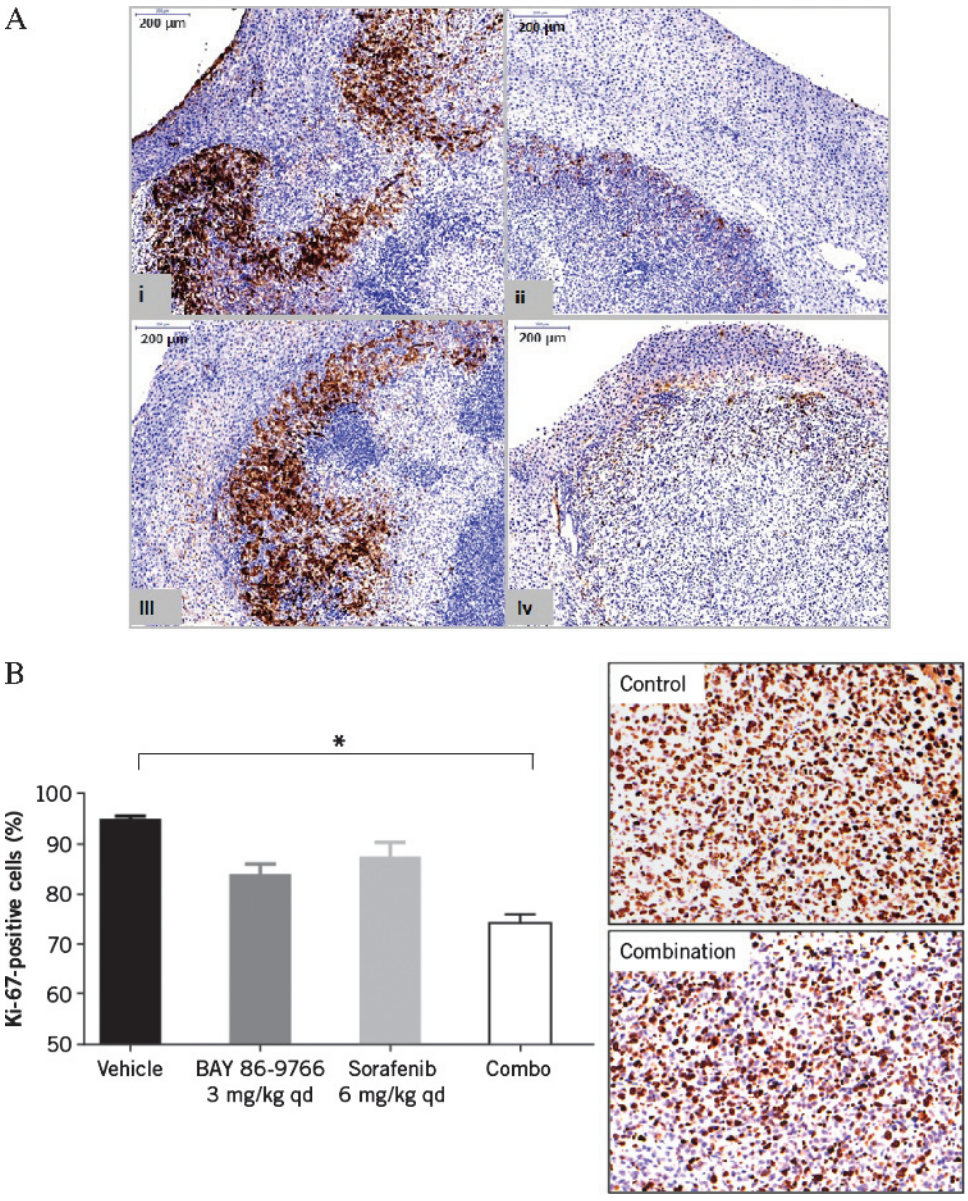

Figure 4. Effect of BAY 86-9766 and sorafenib, as single agents and in combination, in MH3924A cells and MH3924A allografts. Inhibitory effect of BAY 86-9766 on phosphorylation of ERK: pERK staining of liver tumor paraffin sections of animals (A) from (i) vehicle group, (ii) BAY 86-9766 group, (iii) sorafenib group, and (iv) combination group. The proportions of cells staining positive for Ki-67 are shown in B. Inhibitory effect of BAY 86-9766 on angiogenesis with staining with von Willebrand factor is shown in C. Significance is indicated by asterisk ($P < .05$). Kaplan-Meier survival curves and median survival data are shown in D.

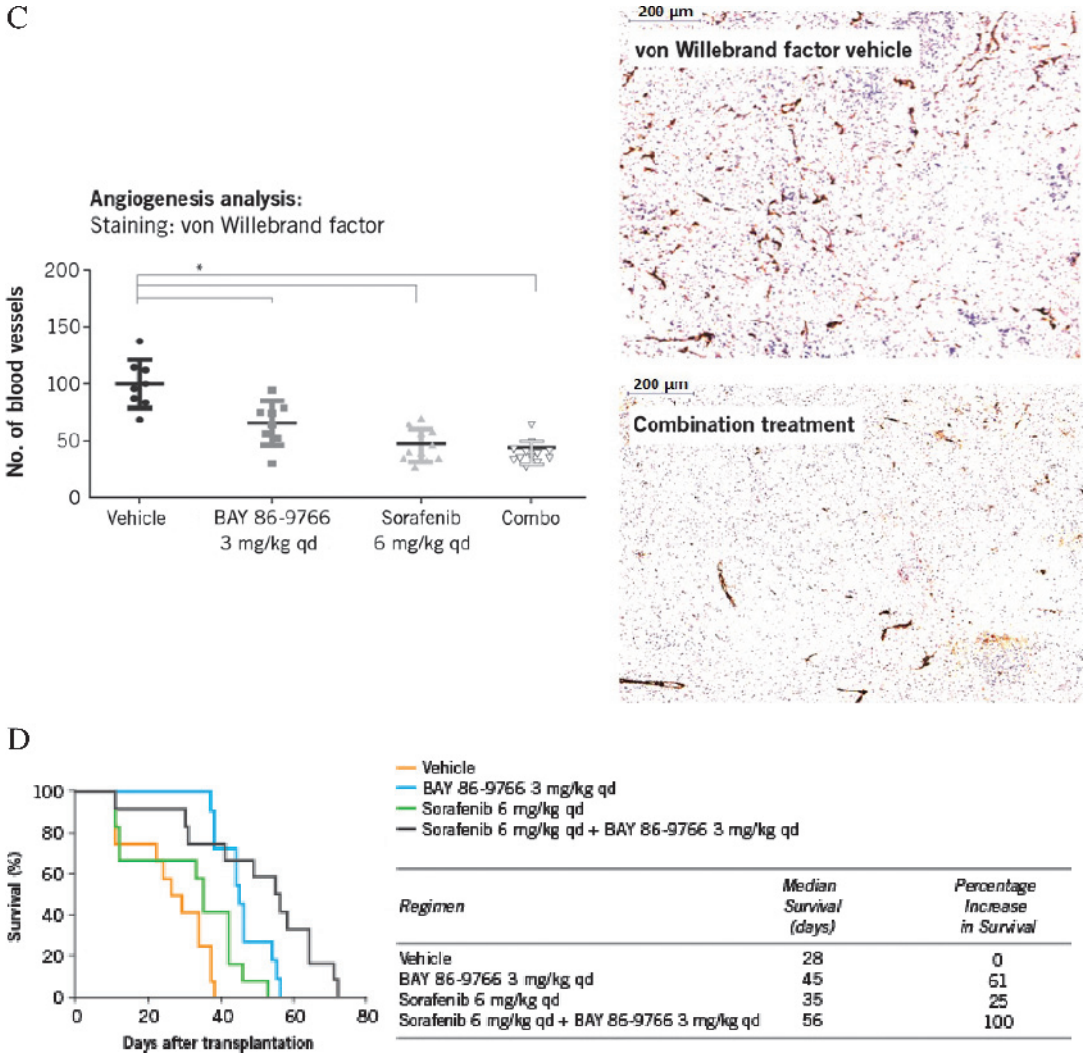

Regimen	*Median Survival (days)*	*Percentage Increase in Survival*
Vehicle	28	0
BAY 86-9766 3 mg/kg qd	45	61
Sorafenib 6 mg/kg qd	35	25
Sorafenib 6 mg/kg qd + BAY 86-9766 3 mg/kg qd	56	100

Figure 4. (*continued*).

groups. BAY 86-9766 and combination therapy, but not sorafenib therapy alone, reduced serum alkaline phosphatase toward levels found in healthy controls, suggesting that BAY 86-9766 protected the animals from intrahepatic cholestasis (Figure 3*D*). Similarly, BAY 86-9766 and combination therapy, but not sorafenib therapy alone, significantly reduced Ki-67 staining in tumor specimens compared with vehicle control ($P < .05$; Figure 4*B*). In the survival analysis, combination therapy prolonged median survival to 56 days, which was greater than the median survival duration of 45 days with single-agent BAY 86-9766 and 35 days with single-agent sorafenib, and double the survival duration seen in the vehicle control group ($P = .008$) after correction for multiple comparisons using the Bonferroni method ($P < .0001$ by the log-rank test; Figure 4*D*).

ERK phosphorylation was examined in MH3924A allograft tumor samples and visualized by Western blot analysis. Treatment with BAY 86-9766, but not sorafenib, inhibited ERK phosphorylation in the tumor lysates (Figure W3). Similarly, BAY 86-9766, as a single-agent and in combination with sorafenib, but not single-agent sorafenib, demonstrated inhibition of ERK activation through pERK immunohistochemistry analysis of liver tumor specimens compared with vehicle control (Figure 4*A*, *i–iv*). Additionally, the effect on tumor blood vessel growth was examined in MH3924A model using IHC staining for von Willebrand factor. The number of tumor blood vessels after treatment with single-agent BAY 86-9766, single-agent sorafenib, and BAY 86-9766 in combination with sorafenib was significantly lower when compared with vehicle control–treated cells (Figure 4*C*). Thus, treatment with both BAY 86-9766 and sorafenib demonstrates statistically significant antiangiogenic effects, which may contribute to the inhibition of tumor growth.

Pharmacokinetic Properties

Plasma concentrations of BAY 86-9766 and sorafenib were measured after 14 days of treatment with 3 and 6 mg/kg once daily (qd) respectively, in rats with MH3924A allografts (Figure 5). Plasma concentrations of BAY 86-9766 show only small changes within a dosing interval with a peak-trough ratio of about 1.5. The unbound average plasma concentration of BAY 86-9766 was very close to the antiproliferative IC_{50} of the drug against MH3924A cells *in vitro*. Plasma sorafenib levels remained about 60-fold below the drug's *in vitro* antiproliferative IC_{50} against MH3924A but were closer to the IC_{50} against human umbilical vein endothelial cells. The C_{max} and $AUC_{0–24}$ of both compounds did not significantly differ between single compound administration and combination treatment.

Discussion

Sorafenib is the current standard of care for patients with advanced HCC who have preserved liver function [24]. In two randomized controlled phase III trials, sorafenib significantly extended survival compared with placebo; however, median OS in the sorafenib arms of both studies modestly increased [22,23]. As a result, there is a need for new and effective HCC treatments capable of further improving patient outcome.

MEK is an attractive therapeutic target because 1) MEK and its downstream target, ERK, are frequently overexpressed in HCC, which correlates with disease progression [13,15]; 2) endogenous inhibitors of the MAPK pathway, including Raf-1 kinase inhibitory protein and Spred-1, are frequently downregulated, resulting in increased MEK/ERK activity [8,12]; 3) increased signaling through the MAPK pathway results in cellular proliferation, survival, differentiation, migration, and angiogenesis [5–7]; and 4) pathway activation has been observed after HBV and HCV infection and under chronic alcohol abuse. BAY 86-9766 is an orally available small molecule that binds to an allosteric region adjacent to the ATP-binding pocket of MEK and inhibits both MEK 1 and MEK 2 with high potency and selectivity.

The present experimental studies evaluated whether BAY 86-9766 acts synergistically with sorafenib to block cell proliferation *in vitro* and inhibit tumor growth, metastatic spread, and relevant complications (e.g., ascites, cholestasis) and prolong survival *in vivo*. The models covered a wide range of HCC subtypes, including virus-induced and chemical-induced etiologies. To study the efficacy of BAY 86-9766 in a natural tumor microenvironment, three of the four cell lines were implanted orthotopically. For comparison, the combination of BAY 86-9766 and sorafenib was also tested in the Huh-7 subcutaneous standard xenograft model.

BAY 86-9766 showed potent antiproliferative activity *in vitro* in each of the HCC cell lines evaluated. Moreover, BAY 86-9766 in combination with sorafenib showed strong synergistic effects in suppressing tumor cell proliferation in both human Hep3B cells and rat MH3924A cells. In these cell lines, the strongest synergistic effect was seen when the molar concentration of BAY 86-9766 was either the same as or approximately two-fold lower than the sorafenib concentration. Synergistic effects also occur in terms of blocking the MAPK pathway. Due to combination treatment, compensatory feedback mechanisms regarding up-regulation of phosphorylated MEK after BAY 86-9766 monotreatment were diminished and the phosphorylation of ERK was more potently blocked over a longer period (12 hours) compared to monotherapy in MH3924A cells. It has been described that activated ERK phosphorylates and inhibits CRAF kinase and the inhibition of ERK signaling by allosteric MEK inhibitors relieves ERK-dependent feedback inhibition of CRAF and induces MEK phosphorylation in most cells [30–32]. Our hypothesis is that this mode of action for pMEK feedback regulation is also true for BAY 86-9766. Single-agent sorafenib showed comparable effects with single-agent BAY 86-9766 in blocking pERK when MH3924A cells were incubated with high concentrations of 10 μM. Single-agent BAY 86-9766 and combination therapy with sorafenib effectively inhibited pERK signaling in MH3924A allograft models. Contrary to our cellular experiments, *in vivo* tumor lysates and immunologic staining showed no inhibitory effect of sorafenib on phosphorylation of ERK. It is described that Raf inhibitors (like sorafenib) increase, in BRAF wild-type cells, the phosphorylation of downstream effectors MEK and ERK at low concentrations (paradoxical activation) and inhibit the pathway at highest concentration (biphasic regulation) [33,34]. This is exactly the situation we face in our *in vitro* and *in vivo* studies. The cell line MH3924A is incubated with a very high sorafenib concentration, and pERK reduction could be observed in the cells. In the MH3924A allograft model, the plasma sorafenib levels remained about 60-fold below the cellular IC_{50}, and as expected, pERK activation is detected in the MH3924A tumors at these low sorafenib concentrations.

A

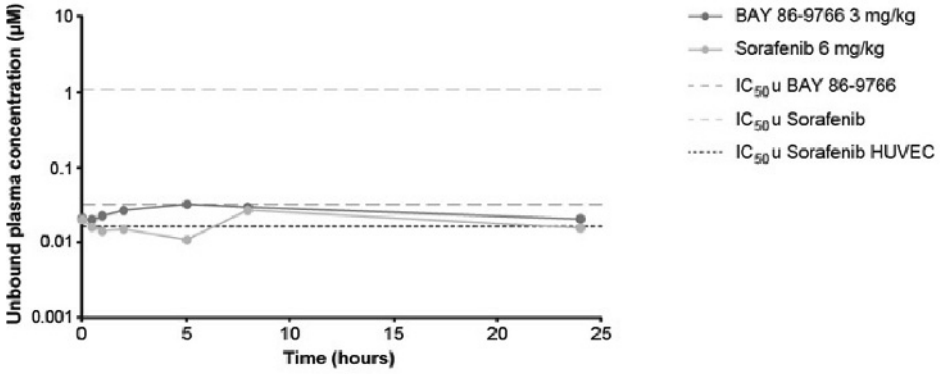

B

	BAY 86-9766		Sorafenib	
	Single Agent	Combination	Single Agent	Combination
$AUC(0\text{-}24)_{norm}$ [kg•h/L]	119	118	12	9
$C_{max,norm}$ [kg/L]	6.92	5.99	0.69	0.53

Figure 5. Pharmacokinetics of BAY 86-9766 and sorafenib in rats with orthotopic MH3924A allografts. Unbound plasma concentration–time curves after last dose of combined treatment with 3 mg/kg qd BAY 86-9766 and 6 mg/kg qd sorafenib (given 5.75 hours later) are shown in A, with the horizontal lines depicting the IC_{50} values of the respective drugs in the MH3924A cells *in vitro*. Pharmacokinetic parameters for each drug individually and in combination are shown in B.

BAY 86-9766 also demonstrated potent antitumor activity in the xenograft and allograft models. As a single agent, BAY 86-9766 inhibited tumor growth in the human Huh-7 HCC xenograft model, prolonged survival and reduced serum AFP levels in the human Hep3B HCC xenograft model, and prolonged survival in the murine Hepa129 allograft model. In the rat MH3924A allograft model, BAY 86-9766 monotherapy reduced tumor growth and ascites formation, protected against cholestasis, and prolonged survival. Positive effects on metastatic spread could be achieved through sorafenib monotherapy and combination therapy. When given in combination, BAY 86-9766 and sorafenib acted synergistically in reducing tumor growth and prolonging survival in multiple models, including the human Hep3B HCC xenograft and the rat MH3924A allograft.

Combination of BAY 86-9766 with sorafenib may achieve synergistic activity in two ways, namely, 1) blockade of the MAPK pathway at two different points (RAF with sorafenib and MEK with BAY 86-9766) or 2) blockade of parallel signaling pathways (blocking the MAPK pathway with BAY 86-9766 and blocking VEGFR-mediated signaling pathways with sorafenib). Evidence favoring the first possibility has been reported in melanoma cells where the combination of a BRAF inhibitor and MEK inhibitor enhanced apoptosis and prevented the onset of resistance [35]. Additionally, our findings demonstrated that both BAY 86-9766 and sorafenib monotherapies, as well as BAY 86-9766 + sorafenib combination therapy, had significant antiangiogenic effects in the MH3924A HCC model.

Tumor blood vessel formation was inhibited by single-agent BAY 86-9766, single-agent sorafenib, and BAY 86-9766 in combination with sorafenib. BAY 86-9766 monotherapy also effectively inhibited pERK signaling. Together, these data provide evidence that sorafenib and BAY 86-9766 are acting synergistically by blocking parallel signal pathways; sorafenib is primarily blocking VEGFR-mediated signaling, while BAY 86-9766 acts directly on the MAPK pathway *in vitro* and *in vivo*.

The rat MH3924A allograft model may shed some light on the mechanism for *in vivo* synergism between BAY 86-9766 and sorafenib. Throughout the 24-hour dosing level, plasma BAY 86-9766 concentrations remained close to the drug's antiproliferative IC_{50} against MH3924A cells. These findings suggest that the efficacy of BAY 86-9766 results from a direct effect on the tumor cells. Although plasma sorafenib concentrations remained below its antiproliferative IC_{50} against tumor cells, it was close to its IC_{50} against endothelial cells, thereby suggesting that the efficacy of sorafenib may be due to an indirect effect. Taken together, the antiproliferative effect of BAY 86-9766 and the antiangiogenic properties of sorafenib might combine in the MH3924A *in vivo* model to produce a synergistic antitumoral effect. Nevertheless, our *in vitro* combination experiments also indicate a direct synergistic antiproliferative effect between BAY 86-9766 and sorafenib in MH3924A tumor cells.

In summary, the models used in these investigations cover multiple HCC subtypes, including virus-induced and chemical-induced etiologies. Even in tumor models that show less potent antiproliferative IC_{50} values *in vitro* than the NRAS-mutated HepG2 cell line, BAY 86-9766 showed great *in vivo* potency, which emphasizes the effectiveness of the MEK inhibitor.

The role of the tumor stroma and immunologic interactions was addressed by the orthotopical transplantation of the allograft cells in the liver and the inclusion of two models with immunocompetent animals.

Antitumor efficacy of BAY 86-9766, particularly when used in combination with sorafenib, was observed in each model, suggesting that this novel MEK inhibitor has potential for broad usage across multiple HCC subtypes. BAY 86-9766 exhibited significant single-agent antitumor activity, but MEK inhibitor monotherapy may not be sufficient for clinical efficacy in a variety of clinical settings. In a recent phase II trial, a different MEK inhibitor, selumetinib (AZD 6244), did not produce radiographic responses in patients with advanced HCC even though there was evidence of ERK inhibition [36]. The potent synergism observed between BAY 86-9766 and sorafenib suggests that a combination therapy approach may be a more promising addition to treatment of HCC. Along these lines, the results of a phase II clinical trial (NCT01204177) [37] investigating BAY 86-9766 (50 mg, twice a day) in combination with sorafenib (400 mg, twice a day) as first-line treatment for patients with advanced HCC will soon be submitted for publication [37,38].

References

[1] Venook AP, Papandreou C, Furuse J, and de Guevara LL (2010). The incidence and epidemiology of hepatocellular carcinoma: a global and regional perspective. *Oncologist* **15**(suppl 4), 5–13.

[2] Jemal A, Bray F, Center MM, Ferlay J, Ward E, and Forman D (2011). Global cancer statistics. *CA Cancer J Clin* **61**, 69–90.

[3] Ma YT and Palmer DH (2012). Impact of restricting access to high-cost medications for hepatocellular carcinoma. *Expert Rev Pharmacoecon Outcomes Res* **12**, 465–473.

[4] Olsen SK, Brown RS, and Siegel AB (2010). Hepatocellular carcinoma: review of current treatment with a focus on targeted molecular therapies. *Therap Adv Gastroenterol* **3**, 55–66.

[5] Roberts PJ and Der CJ (2007). Targeting the Raf-MEK-ERK mitogen-activated protein kinase cascade for the treatment of cancer. *Oncogene* **26**, 3291–3310.

[6] Friday BB and Adjei AA (2008). Advances in targeting the Ras/Raf/MEK/Erk mitogen-activated protein kinase cascade with MEK inhibitors for cancer therapy. *Clin Cancer Res* **14**, 342–346.

[7] Fremin C and Meloche S (2010). From basic research to clinical development of MEK1/2 inhibitors for cancer therapy. *J Hematol Oncol* **3**, 8.

[8] Wong CM and Ng IO (2008). Molecular pathogenesis of hepatocellular carcinoma. *Liver Int* **28**, 160–174.

[9] Tannapfel A, Sommerer F, Benicke M, Katalinic A, Uhlmann D, Witzigmann H, Hauss J, and Wittekind C (2003). Mutations of the *BRAF* gene in cholangiocarcinoma but not in hepatocellular carcinoma. *Gut* **52**, 706–712.

[10] Nonomura A, Ohta G, Hayashi M, Izumi R, Watanabe K, Takayanagi N, Mizukami Y, and Matsubara F (1987). Immunohistochemical detection of ras oncogene p21 product in liver cirrhosis and hepatocellular carcinoma. *Am J Gastroenterol* **82**, 512–518.

[11] Jagirdar J, Nonomura A, Patil J, Thor A, and Paronetto F (1989). ras oncogene p21 expression in hepatocellular carcinoma. *J Exp Pathol* **4**, 37–46.

[12] Schuierer MM, Bataille F, Weiss TS, Hellerbrand C, and Bosserhoff AK (2006). Raf kinase inhibitor protein is downregulated in hepatocellular carcinoma. *Oncol Rep* **16**, 451–456.

[13] Schmidt CM, McKillop IH, Cahill PA, and Sitzmann JV (1997). Increased MAPK expression and activity in primary human hepatocellular carcinoma. *Biochem Biophys Res Commun* **236**, 54–58.

[14] Tsuboi Y, Ichida T, Sugitani S, Genda T, Inayoshi J, Takamura M, Matsuda Y, Nomoto M, and Aoyagi Y (2004). Overexpression of extracellular signal-regulated protein kinase and its correlation with proliferation in human hepatocellular carcinoma. *Liver Int* **24**, 432–436.

[15] Ito Y, Sasaki Y, Horimoto M, Wada S, Tanaka Y, Kasahara A, Ueki T, Hirano T, Yamamoto H, Fujimoto J, et al. (1998). Activation of mitogen-activated protein kinases/extracellular signal-regulated kinases in human hepatocellular carcinoma. *Hepatology* **27**, 951–958.

[16] Lupberger J and Hildt E (2007). Hepatitis B virus-induced oncogenesis. *World J Gastroenterol* **13**, 74–81.

[17] Nagy LE (2004). Molecular aspects of alcohol metabolism: transcription factors involved in early ethanol-induced liver injury. *Annu Rev Nutr* **24**, 55–78.

[18] Hennig M, Yip-Schneider MT, Klein P, Wentz S, Matos JM, Doyle C, Choi J, Wu H, O'Mara A, Menze A, et al. (2009). Ethanol-TGFα-MEK signaling promotes growth of human hepatocellular carcinoma. *J Surg Res* **154**, 187–195.

[19] Schmitz KJ, Wohlschlaeger J, Lang H, Sotiropoulos GC, Malago M, Steveling K, Reis H, Cicinnati VR, Schmid KW, and Baba HA (2008). Activation of the ERK and AKT signalling pathway predicts poor prognosis in hepatocellular carcinoma and ERK activation in cancer tissue is associated with hepatitis C virus infection. *J Hepatol* **48**, 83–90.

[20] Wilhelm SM, Carter C, Tang L, Wilkie D, McNabola A, Rong H, Chen C, Zhang X, Vincent P, McHugh M, et al. (2004). BAY 43-9006 exhibits broad spectrum oral antitumor activity and targets the RAF/MEK/ERK pathway and receptor tyrosine kinases involved in tumor progression and angiogenesis. *Cancer Res* **64**, 7099–7109.

[21] Liu PC, Liu X, Li Y, Covington M, Wynn R, Huber R, Hillman M, Yang G, Ellis D, Marando C, et al. (2006). Identification of ADAM10 as a major source of HER2 ectodomain sheddase activity in HER2 overexpressing breast cancer cells. *Cancer Biol Ther* **5**, 657–664.

[22] Llovet JM, Ricci S, Mazzaferro V, Hilgard P, Gane E, Blanc JF, de Oliveira AC, Santoro A, Raoul JL, Forner A, et al. (2008). Sorafenib in advanced hepatocellular carcinoma. *N Engl J Med* **359**, 378–390.

[23] Cheng AL, Kang YK, Chen Z, Tsao CJ, Qin S, Kim JS, Luo R, Feng J, Ye S, Yang TS, et al. (2009). Efficacy and safety of sorafenib in patients in the Asia-Pacific region with advanced hepatocellular carcinoma: a phase III randomised, double-blind, placebo-controlled trial. *Lancet Oncol* **10**, 25–34.

[24] National Comprehensive Cancer Network (NCCN). NCCN Clinical Practice Guidelines in Oncology/Hepatobiliary Cancers v.2004. Available at: http://www.nccn.org/.

[25] Iverson C, Larson G, Lai C, Yeh LT, Dadson C, Weingarten P, Appleby T, Vo T, Maderna A, Vernier JM, et al. (2009). RDEA119/BAY 869766: a potent, selective, allosteric inhibitor of MEK1/2 for the treatment of cancer. *Cancer Res* **69**, 6839–6847.

[26] Jonkers J and Berns A (2002). Conditional mouse models of sporadic cancer. *Nat Rev Cancer* **2**, 251–265.

[27] Killion JJ, Radinsky R, and Fidler IJ (1998). Orthotopic models are necessary to predict therapy of transplantable tumors in mice. *Cancer Metastasis Rev* **17**, 279–284.

[28] Mohandas K (2004). Hepatitis B associated hepatocellular carcinoma: epidemiology, diagnosis and treatment. *Hep B Annual* **1**, 140–152.

[29] Chou TC (2006). Theoretical basis, experimental design, and computerized simulation of synergism and antagonism in drug combination studies. *Pharmacol Rev* **58**, 621–681.

[30] Ishii N, Harada N, Joseph EW, Ohara K, Miura T, Sakamoto H, Matsuda Y, Tomii Y, Tachibana-Kondo Y, Iikura H, et al. (2013). Enhanced inhibition of ERK signaling by a novel allosteric MEK inhibitor, CH5126766, that suppresses feedback reactivation of RAF activity. *Cancer Res* **73**, 4050–4060.

[31] Wang Y, Van Becelaere K, Jiang P, Przybranowski S, Omer C, and Sebolt-Leopold J (2005). A role for K-ras in conferring resistance to the MEK inhibitor, CI-1040. *Neoplasia* **7**, 336–347.

[32] Huynh H, Soo KC, Chow PK, and Tran E (2007). Targeted inhibition of the extracellular signal-regulated kinase kinase pathway with AZD6244 (ARRY-142886) in the treatment of hepatocellular carcinoma. *Mol Cancer Ther* **6**, 138–146.

[33] Poulikakos PI, Zhang C, Bollag G, Shokat KM, and Rosen N (2010). RAF inhibitors transactivate RAF dimers and ERK signalling in cells with wild-type BRAF. *Nature* **18**, 427–430.

[34] Holderfield M, Merritt H, Chan J, Wallroth M, Tandeske L, Zhai H, Tellew J, Hardy S, Hekmat-Nejad M, Stuart DD, et al. (2013). RAF inhibitors activate the MAPK pathway by relieving inhibitory autophosphorylation. *Cancer Cell* **13**, 594–602.

[35] Paraiso KH, Fedorenko IV, Cantini LP, Munko AC, Hall M, Sondak VK, Messina JL, Flaherty KT, and Smalley KS (2010). Recovery of phospho-ERK activity allows melanoma cells to escape from BRAF inhibitor therapy. *Br J Cancer* **102**, 1724–1730.

[36] O'Neil BH, Goff LW, Kauh JS, Strosberg JR, Bekaii-Saab TS, Lee RM, Kazi A, Moore DT, Learoyd M, Lush RM, et al. (2011). Phase II study of the mitogen-activated protein kinase 1/2 inhibitor selumetinib in patients with advanced hepatocellular carcinoma. *J Clin Oncol* **29**, 2350–2356.

[37] U.S. National Institutes of Health. Assessing BAY86-9766 Plus Sorafenib for the Treatment of Liver Cancer (BASIL), 2010. Available at: http://www.clinicaltrials.gov/ct2/show/NCT01204177?term=NCT01204177&rank=1. Accessed October 01, 2013.

[38] Weekes CD, Von Hoff DD, Adjei AA, Leffingwell DP, Eckhardt SG, Gore L, Lewis KD, Weiss GJ, Ramanathan RK, Dy GK, et al. (2013). Multicenter phase I trial of the mitogen-activated protein kinase 1/2 inhibitor BAY 86-9766 in patients with advanced cancer. *Clin Cancer Res* **19**, 1232–1243.

Supplementary Materials and Methods

Western Blot Analysis from MH3924A Cells and Allograft

Western blot analysis. MH3924A cells were treated with BAY 86-9766 (1 μM), sorafenib (10 μM), the combination of both compounds, or medium with 0.1% DMSO for 2, 7, and 12 hours. Cells were washed with cold phosphate-buffered saline and lysed with lysis buffer (MSD, Gaithersburg, MD). Shock-frozen tumor samples from animals of the vehicle and treatment groups from the allograft MH3924A model were lysed as well.

Twenty micrograms of protein was loaded on a Bis-Tris NuPAGE gel (Invitrogen, Carlsbad, CA), electrophoresed, and transferred using iBlot system (Invitrogen) to a polyvinylidenefluoride (PVDF) membrane. Blots were probed with anti-pERK and anti-ERK [phospho-p44/42 MAPK (Thr^{202}/Tyr^{204})/p44/42 MAPK (ERK1/2); Cell Signaling Technology, Inc, Danvers, MA]. Control cell extracts from Cell Signaling Technology [p44/42 MAPK (ERK1/2)] served as positive and negative controls. As a secondary antibody, Alexa Fluor 680 goat anti-rabbit IgG (Invitrogen) was used, and detection took place with the Odyssey Infrared Imaging System.

Immunohistochemistry. Liver tumor tissue from the MH3924A allograft model was fixed in formalin, transferred to ethanol, and embedded in paraffin. Sections of 3 μm were cut, and after deparaffinization, enzymatic antigen retrieval (Dako Proteolytic Enzymes, Carpinteria, CA) was carried out. Primary antibodies were used to detect pERK [phospho-p44/42 MAPK (Thr^{202}/Tyr^{204}); Cell Signaling Technology, Inc], Ki-67 (SP6; Abcam, Cambridge, United Kingdom), and von Willebrand factor (rabbit polyclonal; Abcam). An appropriate isotype control was carried along on every slide.

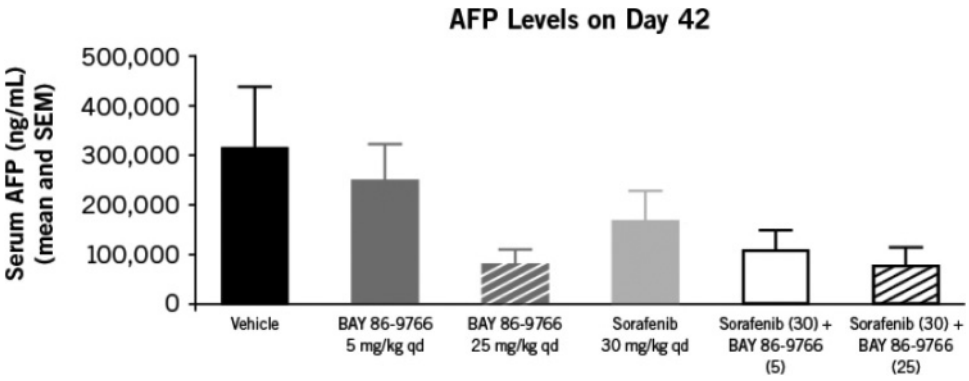

Figure W1. Serum AFP levels were measured on day 42 in the orthotopic HBV-driven human Hep3B xenograft model. Lowest levels of serum AFP levels were seen in the group receiving BAY 86-9766 (25 mg/kg) sorafenib followed by BAY 86-9766 (25 mg/kg) monotherapy.

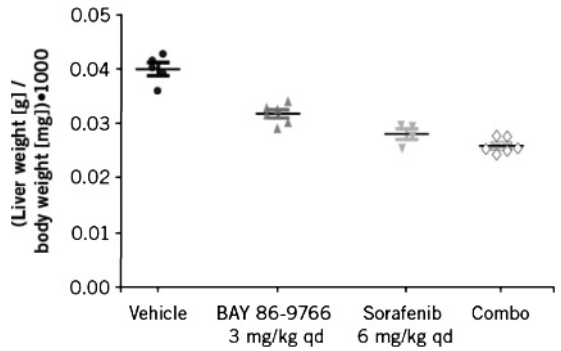

Figure W2. Effect of BAY 86-9766 and sorafenib, as single agents and in combination, on tumor growth of the MH3924A allograft model. The weight of the liver as a percentage of total body weight is shown.

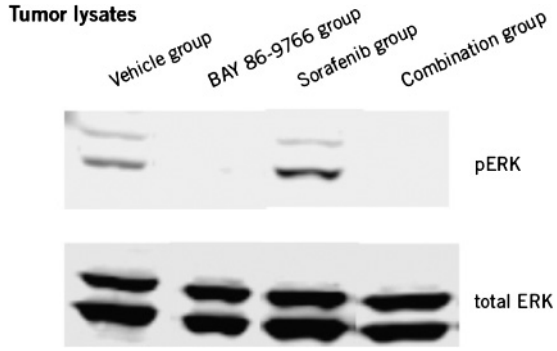

Figure W3. Inhibitory effect of BAY 86-9766 on phosphorylation of ERK: anti-pERK Western blot analysis in MH3924A allografts.